



Investigation of the Microstructure and Mechanical Properties of AZ31/Graphene Composite Fabricated by Semi-solid Isothermal Treatment and Hot Extrusion

ZHAO YANG,¹ HONGYU XU,^{1,2} YE WANG,¹ MAOLIANG HU,¹ and ZESHENG JI¹

1.—School of Materials Science and Engineering, Harbin University of Science and Technology, Harbin 150000, China. 2.—e-mail: xuhongyu@hrbust.edu.cn

Magnesium matrix composites reinforced with 0.3 wt.% graphene were fabricated by semi-solid isothermal treatment using various reheating conditions and hot extrusion. The microstructures of the hot-extruded AZ31/graphene composites were clearly refined, with the finest grain size (7.05 μm) achieved after reheating at 610°C for 30 min. Energy-dispersive x-ray spectroscopy analysis revealed that increasing the reheating temperature promotes diffusion of the solute elements and affects the mechanical properties of the composite. The optimal mechanical properties were achieved after reheating at 620°C for 30 min, with a yield strength of 214.82 MPa and an ultimate tensile strength of 310.79 MPa. The significant improvement in the mechanical properties of the composite was mainly attributed to the refined grain size, uniformly redistributed solute elements, addition of graphene, and close interfacial bonding.

INTRODUCTION

As the lightest structural metal, magnesium (Mg) and its alloys have attracted considerable research attention because of their good recyclability, high specific strength, and damping ability.^{1,2} In particular, AZ31 magnesium alloy has been extensively employed because of its low cost and high corrosion resistance.³ However, its limited strength, relatively low ductility, and low oxidation resistance have restricted its application in the transportation and automobile industries. Recently, several researchers have attempted to fabricate Mg-matrix composites by adding reinforcement phases to achieve superior mechanical properties.^{4–9}

Graphene has attracted interest as one of the most ideal reinforcements for metal matrix composites because of its extraordinary Young's modulus (~ 1 TPa) and excellent mechanical strength (~ 130 GPa).^{10–15} Recently, several preparation methods have been developed for the fabrication of graphene-reinforced Mg-matrix composites, including powder metallurgy,¹ stir casting,¹⁶ pressure casting,¹⁷ and disintegrated melt deposition followed by hot extrusion.¹⁸ However, the composites

prepared using powder metallurgy and hot extrusion have weak interface bonding strengths, which limit the ductility of the composites. In addition, in the casting process, graphene undergoes a chemical reaction with the matrix at high temperature, resulting in a reduction of the interface bond strength.¹⁹ Compared with these preparation methods, semi-solid processing (SSP) is considered a more advanced technology for the manufacture of Mg-matrix/graphene composites with good formability and fewer forming defects owing to the excellent fluidity and adjustable viscosity of semi-solid-state materials.²⁰ The fabrication of Mg-matrix composites using SSP has recently received considerable attention. Yan et al.²¹ applied ultrasonic vibration treatment (UVT) to prepare Mg₂Si/AM60 magnesium composites. They observed that a good semi-solid slurry could be obtained by applying UVT at 620°C for 60 s, with Mg₂Si and Mg₁₇Al₁₂ located along the grain boundaries or uniformly dispersed in the matrix with a net-like structure. Chen et al.²² studied SSP of SiC_p/ZM6 magnesium composites. They reported that the microstructure of the composite prepared by recrystallization and partial melting consisted of fine and spheroidal solid

grains surrounded by an intergranular liquid. Yi et al.²⁰ showed that the presence of SiC_p in SiC_p/AZ91 results in lower liquid fractions of semi-solid slurries and yields higher values of flow stress during semi-solid compression testing. However, SSP has not yet been broadly applied for the fabrication of Mg-matrix/graphene composites.

In this work, magnesium matrix composites reinforced with 0.3 wt.% graphene were synthesized by semi-solid isothermal treatment (SSIT) and hot extrusion. The effects of the reheating temperature and holding time on the microstructural evolution and mechanical properties were experimentally investigated, and the strengthening mechanism of the AZ31/graphene composite is discussed in detail.

EXPERIMENTAL PROCEDURE

Materials

AZ31 magnesium alloy chips with the composition of 2.80% Al, 1.00% Zn, and 0.25% Mn (in wt.%) were produced by machining an AZ31 magnesium alloy ingot in a lathe. The chip dimensions were 3.350–4.750 mm × 1.400–2.360 mm × 0.090–0.500 mm. The reinforcement material, graphene, with an average thickness of < 7 nm and purity of ≥ 99 wt.%, was reduced from graphene oxide,²³ which was synthesized using a modified Hummers' method; a detailed description of the preparation

method is provided by Gao et al.²⁴ The microstructure of the raw graphene is shown in Fig. 1a.

Methods

Figure 1b presents a schematic illustration of the preparation process of the AZ31/graphene composite. First, the mixture of AZ31 chips and graphene was prepared by mechanical ball milling with stainless steel balls at 400 rpm for 0.5 h. The weight ratio of the balls to powder was 8:1. Second, 50 g of the AZ31 chips and graphene mixture was pre-heated in a resistance furnace at 633 K for 10 min and then pressed into a 40-mm-diameter cylindrical billet. Third, the cylindrical billet was semi-solid isothermally treated in the furnace under a purified CO₂ atmosphere. After the target temperature and time were reached, the billet was rapidly poured into water to maintain the semi-solid microstructure. The technological parameters of SSIT are given in Table I. Finally, the billet after SSIT was hot-extruded into a rod-like material at 673 K with an extrusion ratio of 25:1 using an extrusion rate of 0.2 mm/s.

The microstructure of the composite was examined using optical microscopy (OM; OLYMPUS-GX71-6230A). The elemental distribution of the composite was determined using scanning electron microscopy (SEM; FEI-SIRION) coupled with

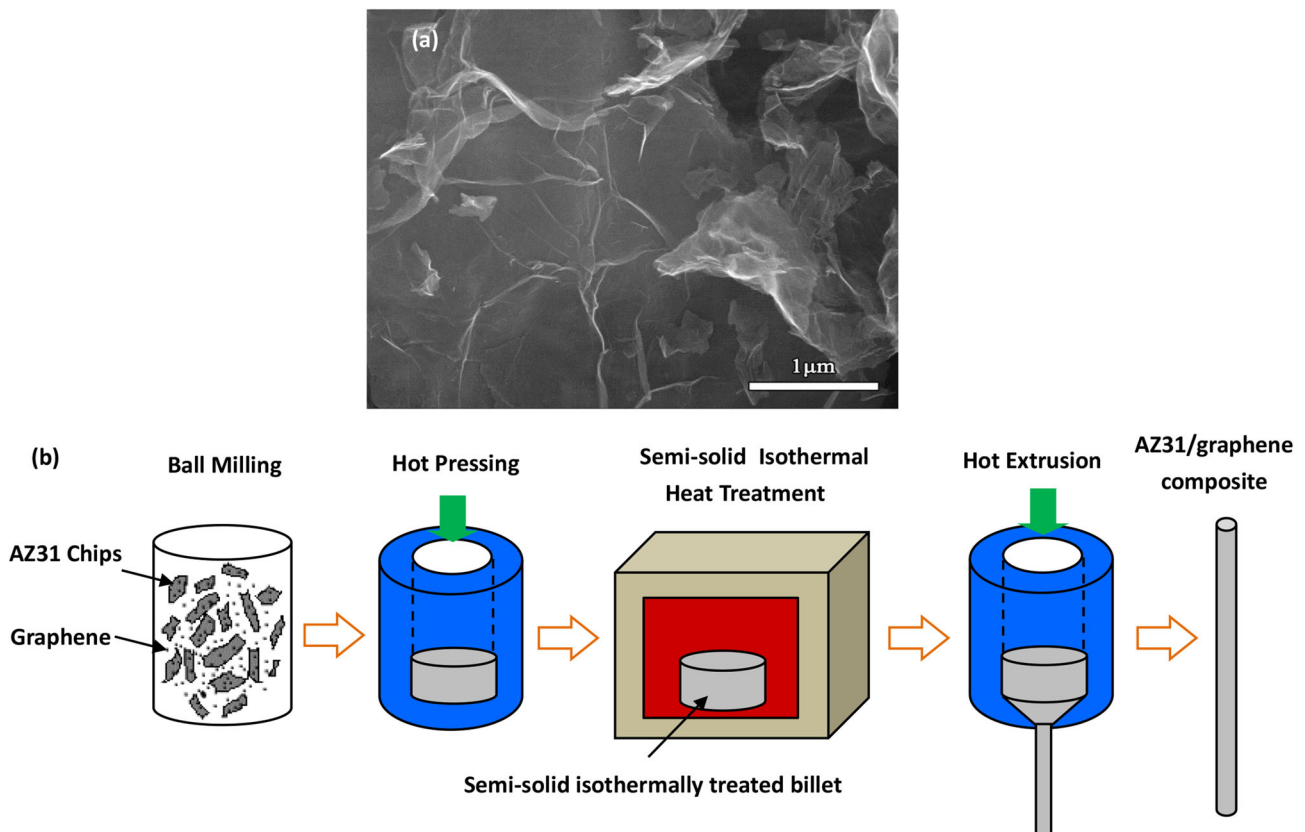


Fig. 1. (a) SEM image of graphene and (b) schematic display of the preparation process for the AZ31/graphene composite.

Table I. Technological parameters of SSIT

Reheating temperature (°C)	Holding time (min)
590	30
600	30
610	10, 20, 30, 40
620	30

energy-dispersive x-ray spectroscopy (EDS). The interface between the graphene and the AZ31 magnesium alloy was examined using transmission electron microscopy (TEM; JEOL JEM-2100). Tensile testing was performed using a universal testing machine (Instron 5500R) at a speed of 0.5 mm/min.

RESULTS AND DISCUSSION

Morphological and Microstructural Analysis

Figure 2a, c, e, and g shows the microstructures of the AZ31/graphene composites after SSIT at various temperatures for 30 min. As observed in Fig. 2a, for a reheating temperature of 590°C, independent and near-spheroidal α -Mg grains were formed, net-shaped eutectic components were observed along the grain boundaries of α -Mg, and graphene was embedded in the eutectic components. Upon increasing the reheating temperature to 600°C, the α -Mg grains were surrounded by an intergranular liquid, with the appearance of some spheroidal and independent grains (Fig. 2c). As observed in Fig. 2e, at 610°C, as the diffusion speed of solute atoms increased, the distribution of graphene became wider under the effect of the increasing volume of the eutectic components. In addition, the spheroidization rate of the α -Mg grains was reduced by the eutectic components inside the α -Mg grains. Upon increasing the reheating temperature to 620°C, the α -Mg grains were basically melted and the graphene distribution range was not pronounced.

To improve the density and mechanical properties of the composite, post-treatment is necessary. In the current study, hot extrusion was used for the post-treatment process. Figure 2b, d, f, and h shows the microstructures of the hot-extruded AZ31/graphene composites. Compared with the grain sizes of the composites after SSIT, those of the composites after hot extrusion were clearly refined. As observed in the insets in Fig. 2b, d, f, and h, the average grain sizes of the hot-extruded AZ31/graphene composites were approximately 9.78 μm , 8.90 μm , 7.05 μm , and 7.36 μm after reheating for 30 min at 590°C, 600°C, 610°C, and 620°C, respectively. Based on the grain-boundary strengthening mechanism, the volume fraction of grain boundaries increases with increasing number of grains, leading to an increase of the strength of the metal. Thus, the reheating

temperature plays an important role in grain boundary strengthening.

Figure 3a, c, e, and g shows the microstructures of the AZ31/graphene composites after SSIT at 610°C for various holding times. As observed in Fig. 3a, after a short holding time, partial melting of the grain boundaries occurred, and the adjacent α -Mg grains were surrounded by networks of eutectic components. Upon increasing the holding time to 20 min (Fig. 3c), the fraction of eutectic components clearly increased, and the α -Mg grains became coarse and separated from others under the effect of liquid penetration. As observed in Fig. 3e, upon increasing the holding time to 30 min, the fraction of eutectic components continued to increase and the α -Mg phase showed no obvious growth tendency. As shown in Fig. 3g, the spheroidal reaction of α -Mg grains was satisfactory after the holding time was increased to 40 min, with the α -Mg grains becoming increasingly spherical and coarse, and the liquid phase content increasing.

Figure 3b, d, f, and h shows the microstructures of the hot-extruded AZ31/graphene composites. Upon increasing the holding time from 10 min to 30 min (Fig. 3b, d, and f), the grain size decreased from 12.66 μm to 7.05 μm . As shown in the insets, the grain size distribution range shrunk and the degree of concentration increased with increasing holding time. When the holding time was further increased from 30 min to 40 min, the grain size increased (Fig. 3h); however, this grain size was still refined compared with that of the composite reheated at 610°C for 10 min. These results indicate that the holding time has a significant effect on the grain refinement of the matrix.

Dynamic recrystallization is known to occur in magnesium alloys during high-temperature deformation. The dynamic recrystallization grain size is affected by the original grain size, the addition of a second phase, and the solute atom distribution in the alloy. Refinement of the original grain size results in more grain boundaries, which are generally favorable areas for recrystallization nucleation; therefore, grain refinement provides more nucleation sites and promotes recrystallization. However, with increasing holding time, the solid grains become coarse; thus, increasing the holding time is unfavorable for refining recrystallization grains. During the recrystallization process, graphene with an ultra-thin 2D structure not only provides numerous nucleation sites but also prevents grain boundary sliding and retards the rate of grain growth. However, the interaction between the solute atoms and grain boundaries hinders dislocation motion and grain boundary migration, resulting in a restriction of grain growth.

Under the effects of these complex factors, the microstructure of the hot-extruded composite was noticeably refined with increasing reheating temperature and holding time. Upon increasing the reheating temperature from 610°C to 620°C (for a

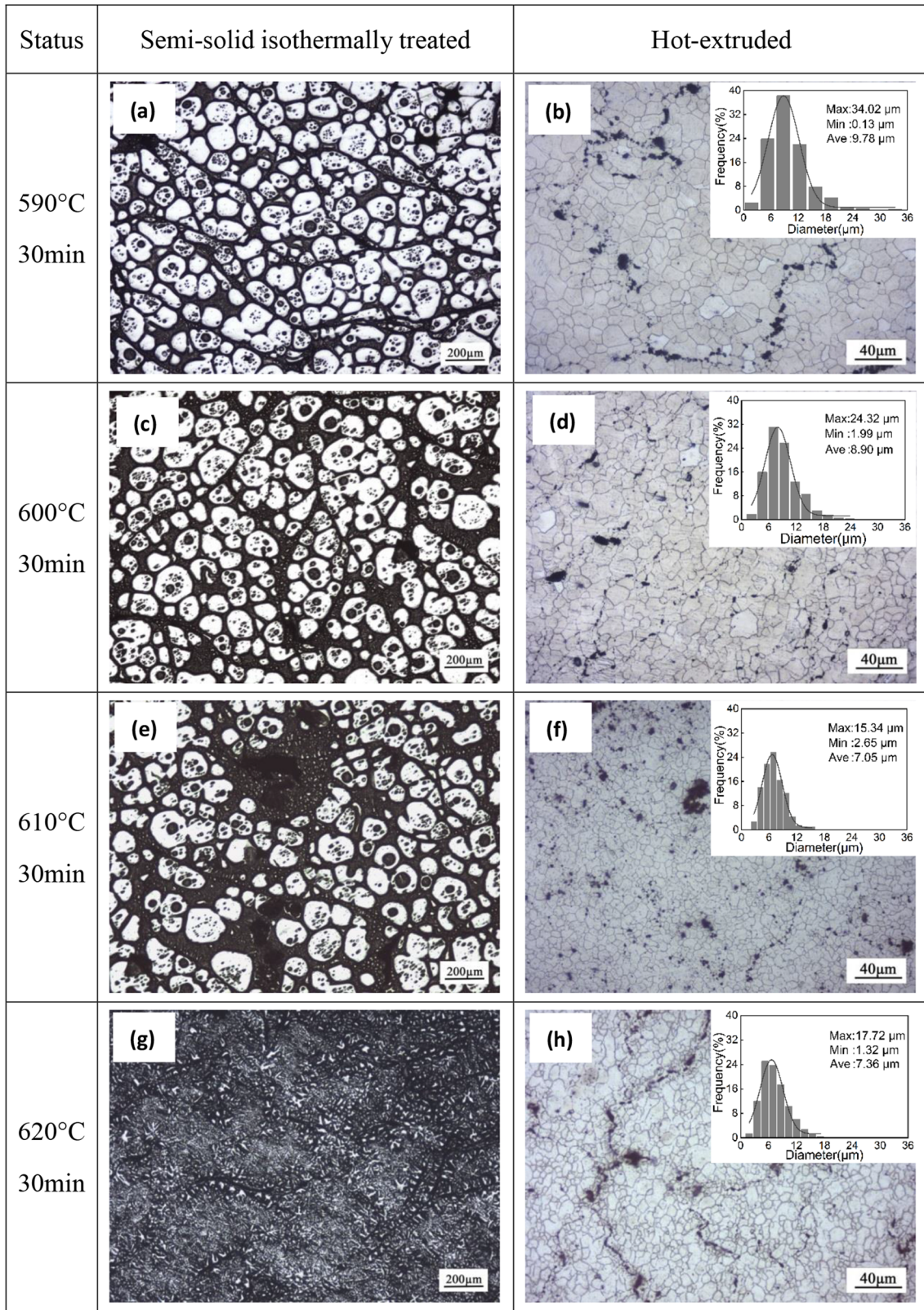


Fig. 2. Microstructures of AZ31/graphene composite after SSIT (a, c, e, g) and hot-extruded microstructures of AZ31/graphene composite (b, d, f, h) after SSIT at various temperatures for 30 min. The grain sizes distribution of the AZ31/graphene composite are displayed in the *inset* and the average grain size values are marked.

Investigation of the Microstructure and Mechanical Properties of AZ31/Graphene Composite Fabricated by Semi-solid Isothermal Treatment and Hot Extrusion

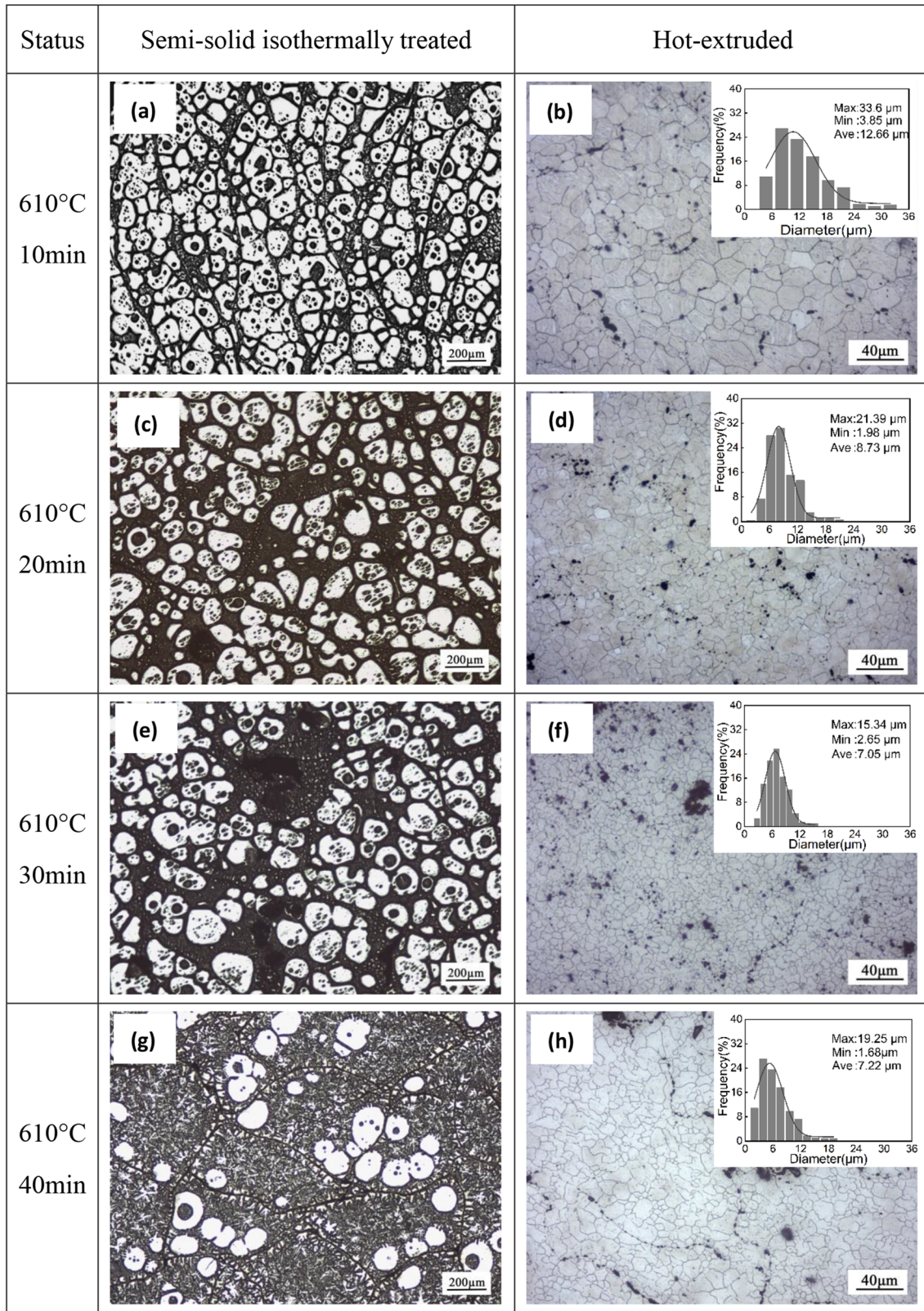


Fig. 3. Microstructures of AZ31/graphene composite after SSIT (a, c, e, g) and hot-extruded microstructures of AZ31/graphene composite (b, d, f, h) after SSIT at 610°C for various holding times. The grain sizes distribution of the AZ31/graphene composite are displayed in the *inset* and the average grain size values are marked.

holding time of 30 min) and increasing the holding time from 30 min to 40 min (for a reheating temperature of 610°C), the grain size of the hot-extruded composite gradually changed.

After SSIT at 590°C and 620°C for 30 min, different segregation conditions of Al and Zn at grain boundaries were observed. Figure 4a and c presents SEM images of the composites after SSIT,

and Fig. 4b and d presents the concentration profiles of Mg, C, Al, and Zn obtained from EDS line scans. The results indicate that the grain boundaries of the matrix were rich in Al and Zn. The maximum Al and Zn concentrations in the solid particles were significantly higher for the composite semi-solid isothermally treated for 30 min at 590°C than at 620°C. In addition, for the latter, the

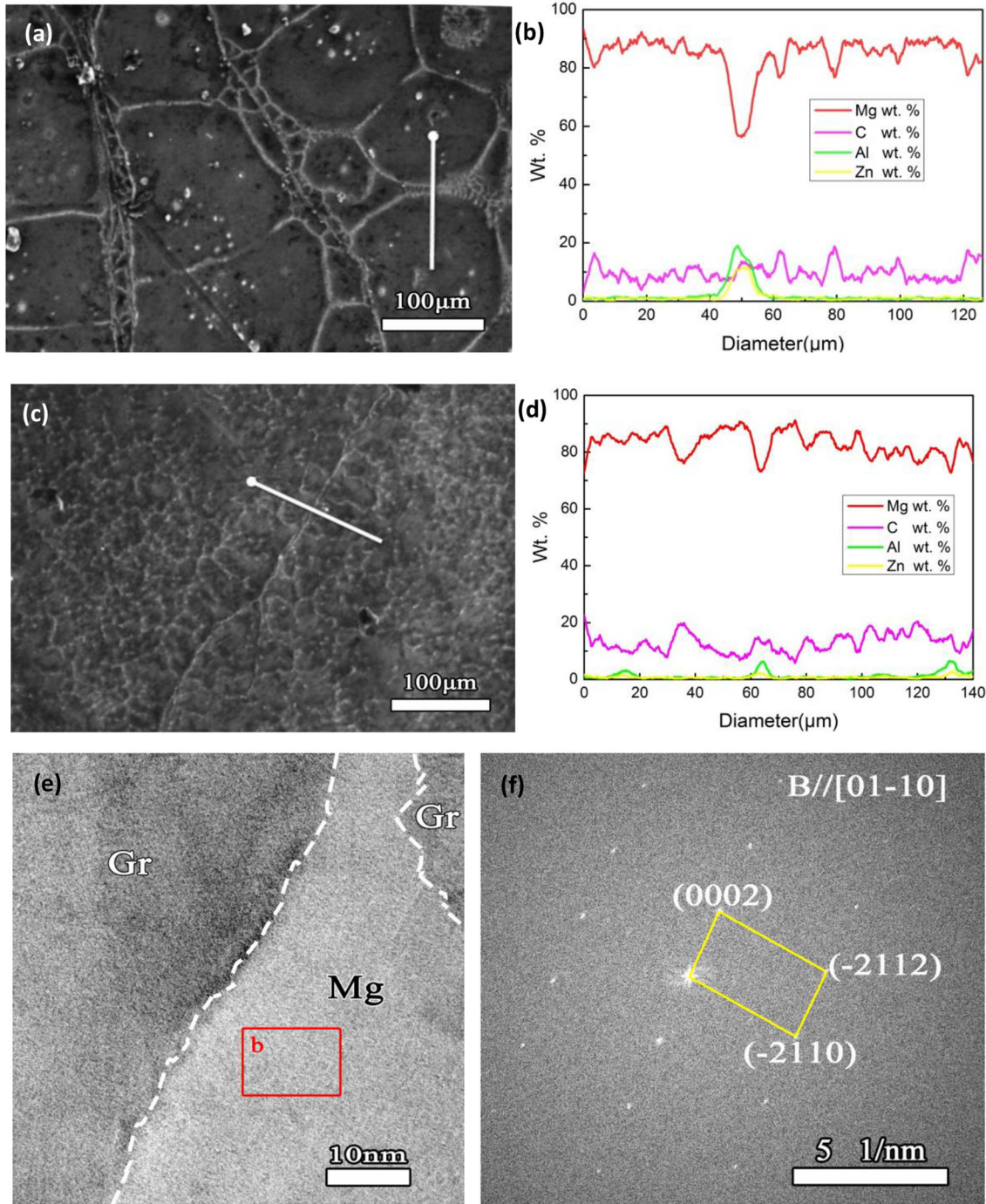


Fig. 4. The morphology and structure of the AZ31/graphene composite. SEM morphology of AZ31/graphene composite after SSIT at 590°C (a) and 620°C (c) for 30 min, and EDS line scan curves showing the distribution of the solutions (b, d). HRTEM of interface structure of the AZ31/graphene composite after SSIT at 620°C for 30 min (e), and (f) diffraction pattern of region b in (e).

measured Al and Zn concentrations in the matrix were smooth. According to Xu's work,²⁵ when the reheating temperature is low, the diffusion of the solute in α -Mg does not result in complete homogenization; therefore, the concentration of the solute at the primary α -Mg grain boundaries is relatively high. With increasing the reheating temperature, the solid particles basically melt and more liquid forms, leading to a uniform distribution of the enriched solute in the matrix.

Figure 4e presents an HRTEM image of the interface structure of the hot-extruded AZ31/graphene composite reheated to 620°C for 30 min, and Fig. 4f presents the corresponding selected area electron diffraction (SAED) patterns obtained from region b in Fig. 4e. According to the corresponding SAED pattern, the lattice constant of the phase with close-packed hexagonal structure (HCP) was $a \sim 0.225$ nm, $b \sim 0.45$ nm and $c \sim 0.257$ nm, and then the phase was identified to be α -Mg matrix. It can be observed that the graphene was embedded in the alloy matrix. In addition, a clear interface was observed between graphene and the matrix in the composite reheated to 620°C for 30 min, indicating that the graphene was perfectly coherent with the matrix with strong interfacial bonding between it and the matrix.

Mechanical Properties

The engineering stress–strain curves and mechanical properties of the hot-extruded AZ31/graphene composites at different reheating states are presented in Fig. 5 and Table II, respectively. For a holding time of 30 min, the yield strength (YS) of the composite was gradually improved, reaching a maximum of 214.82 MPa for a reheating temperature of 620°C. With increasing

the reheating temperature, the ultimate tensile strength (UTS) of the composite initially decreased and then increased, whereas the failure strain of the composite gradually decreased from 11.36% to 5.99%.

For reheating at 610°C, the YS and the failure strain of the composite first increased and then decreased with increasing holding time. For a holding time of 20 min, the composite exhibited the maximum YS (212.44 MPa), which was approximately 11.49% higher than that of the composite held for 40 min (190.54 MPa). The composite with a holding time of 30 min exhibited the optimal failure strain (8.35%), which was approximately 31.50% higher than the lowest value. In addition, with increasing holding time, an overall upward trend of the UTS of the composites from 275.66 MPa to 294.01 MPa was observed.

SSIT was thus observed to have the following effects on the mechanical properties of the composites: (1) close bonding between the reinforcement and matrix, (2) clear grain refinement of the composite, (3) uniform redistribution of solute elements, and (4) the addition of graphene into the magnesium alloy.

One of the major challenges in the synthesis of Mg-matrix nanocomposites is the inadequate interfacial bonding between reinforcements and the Mg alloy matrix.^{26,27} In the current study, with increasing the reheating temperature and holding time, increasingly more eutectic components emerged, which not only enhanced the interfacial bonding strength by improving the wettability but also led to an increase in the load transfer efficiency from the matrix to the reinforcement.

As observed in Figs. 3 and 4, the grain size of the composite first decreased and then increased with increasing the reheating temperature and holding

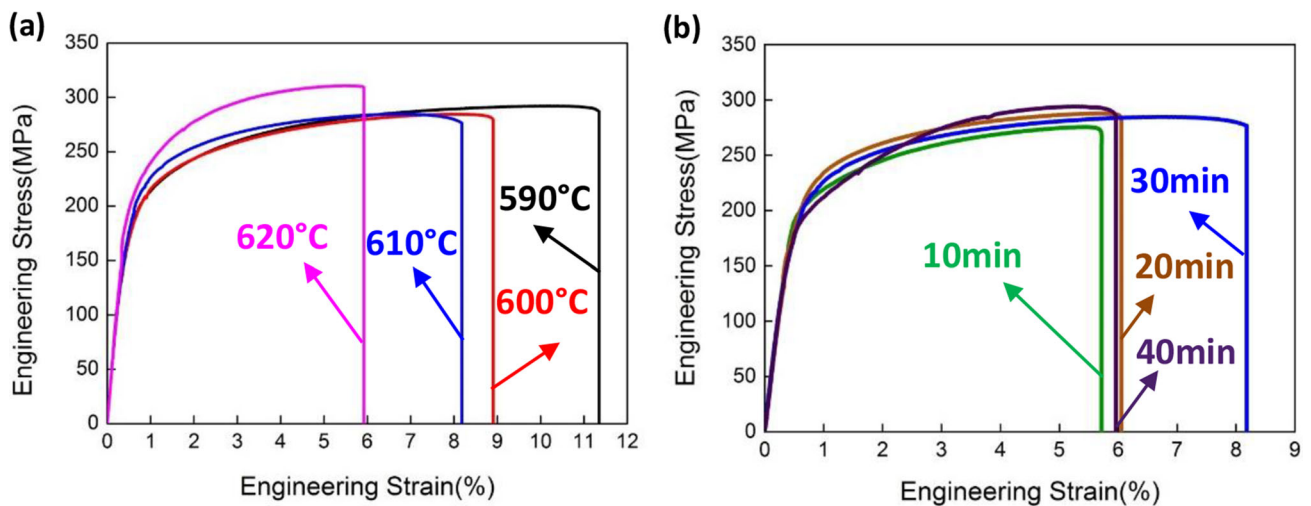


Fig. 5. Engineering stress–strain curves of the AZ31/graphene composite after various reheating temperatures for 30 min (a), and after 610°C for various holding times (b).

Table II. Data of the mechanical properties of the AZ31/graphene composite with various reheating states

Reheating state (°C/min)	YS (MPa)	UTS (MPa)	Failure strain (%)
590/30	184.71 ⁺⁴ ₋₈	292.21 ⁺⁴ ₋₁₀	11.36 ^{+1.2} _{-0.8}
600/30	187.09 ⁺⁹ ₋₇	284.75 ⁺⁵ ₋₈	8.91 ^{+0.9} _{-0.6}
610/10	203.19 ⁺⁴ ₋₆	275.66 ⁺⁷ ₋₅	5.72 ^{+1.5} _{-0.7}
610/20	212.44 ⁺¹² ₋₈	287.82 ⁺⁶ ₋₇	6.06 ^{+0.6} _{-0.7}
610/30	204.89 ⁺⁷ ₋₂	284.73 ⁺⁴ ₋₉	8.35 ^{+0.7} _{-1.3}
610/40	190.54 ⁺⁸ ₋₃	294.01 ⁺³ ₋₉	5.96 ^{+0.4} _{-1.5}
620/30	214.82 ⁺⁷ ₋₃	310.79 ⁺⁸ ₋₁₁	5.99 ^{+0.7} _{-1.1}

time. According to the classical Hall–Petch relationship, $\sigma_y = \sigma_0 + K_y d^{-1/2}$, the mean grain size significantly affects the YS. Zhang et al.²⁸ reported that the reduced grain size provides abundant grain boundaries, which may act as obstacles for the spread of strain from grain to grain, resulting in the improvement of the UTS. When the composite was semi-solid isothermally treated at 610°C for 30 min, the grain size of the composite reached a minimum (7.05 μm). However, the observed variation of the YS and UTS was not as expected from the grain size. This result can be attributed to the significant segregation of Al and Zn induced by SSIT. The atomic radius of Mg (0.160 nm) is larger than that of Zn (0.134 nm) and Al (0.143 nm); therefore, substitution of Mg by Zn and Al leads to a negative misfit. Zeng et al.²⁹ reported that the segregation of solute atoms to the extension region of the dislocation core in the grain boundaries is expected to decrease the elastic strains of the dislocation in the boundaries, thermodynamically reduce the boundary energy, and enhance boundary cohesion. In addition, some studies have shown that the addition of Al and Zn increases the critical resolved shear stress for prismatic $\langle a \rangle$ dislocation slip of AZ31 from 40–50 MPa to 90–100 MPa.^{30–33} Therefore, the solute segregation may negatively affect the mechanical properties.

The enhanced tensile strength of the composite can also be attributed to the addition of graphene. First, the coefficients of thermal expansion (CTEs) of graphene and AZ31 are $1 \times 10^{-6} \text{ K}^{-1}$ and $25 \times 10^{-6} \text{ K}^{-1}$, respectively. This sharp difference in the CTEs of the reinforcement and the matrix may lead to dislocation multiplication at the interface and cause an increase in the YS of composite. The increase of the YS resulting from thermal mismatch can be expressed as^{34,35}

$$\Delta\sigma_{\text{CET}} = \alpha G b \sqrt{\frac{12\Delta T \Delta C f_v}{bd}}$$

where α is a geometric constant, G the shear modulus of the Mg matrix, b the Burgers vector of the Mg matrix, ΔT the difference between the extrusion and testing temperatures, ΔC the difference between the CTE of the matrix and reinforcement, and f_v and d are the volume fraction and

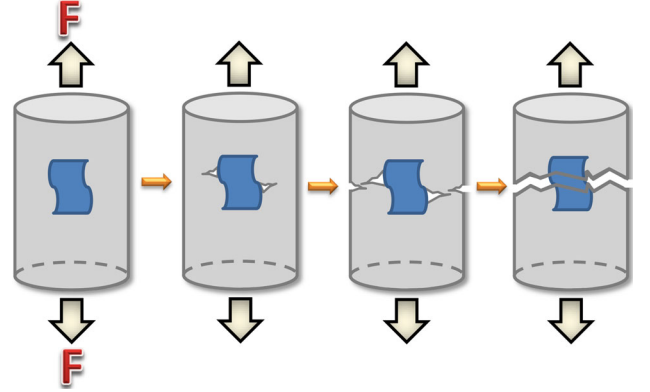


Fig. 6. Schematic of the fracture evolution behaviors of the composite during tensile testing.

average diameter of the reinforcement, respectively. Moreover, the reinforcement will restrict the movement of dislocations, increasing their density and resulting in dislocation strengthening.¹ Second, as observed in Fig. 6, load transfer between the matrix and reinforcement also affects the mechanical properties of the composite. When a tensile force is applied along the extrusion direction of the composite, the load is initially applied to the matrix and then transferred from the matrix to the reinforcement through shear stresses at the interface. The high specific surface area of graphene results in a large contact area between it and the matrix, which leads to an increase in the number of load-transfer sites and provides resistance against tensile fracture. Therefore, the strength of the composite is enhanced.

In addition, with increasing the reheating temperature and holding time, the fraction of the liquid phase increases, which contributes to filling pores between the Mg matrix and reinforcements, enhances the feeding ability to solidification shrinkage during SSIT, and optimizes the plasticity. However, upon further increasing the reheating temperature and holding time, the solidification behavior of the composite becomes similar to that of the full liquid melt; thus, more voids and inclusions are easily formed in the secondary solidified regions, leading to deterioration of the plasticity.³⁶ Thus, the reheating temperature and holding time

substantially affect the failure strain of AZ31/graphene composites.

The results of this study provide a pathway for the fabrication of AZ31/graphene composites with refined grains, enhanced strength, and good particle interfaces. However, additional work is necessary to determine the optimum reheating temperature and holding time to further enhance the properties of Mg-matrix composites.

SUMMARY

AZ31/graphene composites were successfully fabricated using SSIT and hot extrusion, and the reheating temperature and holding time were observed to significantly affect the microstructure and mechanical properties of the composites. Increasing the reheating temperature and holding time greatly refined the grains of the matrix of the AZ31/graphene composite. When the composite was reheated at 610°C and held for 30 min, the grain size of the composite reached a minimum (7.05 μm). In addition, the segregation conditions of Al and Zn at the grain boundaries were improved upon increasing the reheating temperature from 590°C to 620°C. The composite reheated at 620°C and held for 30 min exhibited the optimal mechanical properties (YS = 214.82 MPa and UTS = 310.79 MPa). The increased mechanical strength of the composite was attributed to (1) the close bonding between graphene and the Mg matrix, (2) the refined grain size of the composite, (3) the uniformly redistributed solute elements, and (4) the addition of graphene.

ACKNOWLEDGEMENTS

This work was supported by the National Natural Science Foundation of China (Nos. 51704087 and 51574100) and University Nursing Program for Young Scholars with Creative Talents in Heilongjiang Province (UNPYSCT-2016033).

REFERENCES

1. Q.H. Yuan, G.H. Zhou, L. Lin, L. Yong, and L. Lan, *Carbon* 127, 177 (2018).
2. Y. Ali, D. Qiu, B. Jiang, F.S. Pan, and M.X. Zhang, *J. Alloys Compd.* 619, 639 (2015).
3. M. Rashad, F.S. Pan, J.Y. Zhang, and M. Asif, *J. Alloys Compd.* 646, 223 (2015).
4. Q. Chen, Y. Meng, Y.S. Yi, Y.Y. Wan, S. Sugiyama, and J. Yanagimoto, *J. Alloys Compd.* 774, 93 (2019).
5. I. Dinaharan, S.C. Vettivel, M. Balakrishnan, and E.T. Akinlabi, *J. Magnes. Alloys* 7, 155 (2019).
6. W.B. Yu, X.B. Li, M. Vallet, and L. Tian, *Mech. Mater.* 129, 246 (2019).
7. F. Khorasani, M. Emamy, M. Malekan, H. Mirzadeh, B. Pourbahari, T. Krajnák, and P. Minárik, *Mater. Charact.* 147, 155 (2019).
8. S.T. Manige, G. Harinath Gowd, and B. Chandra Mohan Reddy, *J. Thin Films Coat. Sci. Technol. Appl.* 5, 21 (2018).
9. N. Barri, A.R. Salasel, A. Abbasi, H. Mirzadeh, M. Emamy, and M. Malekan, *Vacuum* 164, 349 (2019).
10. M. Bastwros, G.Y. Kim, C. Zhu, K. Zhang, S. Wang, X.D. Tang, and X.W. Wang, *Compos. B Eng.* 60, 111 (2014).
11. F.Y. Chen, J.M. Ying, Y.F. Wang, S.Y. Du, Z.P. Liu, and Q. Huang, *Carbon* 96, 836 (2016).
12. Z. Li, Q. Guo, Z.Q. Li, G.L. Fan, D.B. Xiong, Y.S. Su, J. Zhang, and D. Zhang, *Nano Lett.* 15, 8077 (2015).
13. D.B. Xiong, M. Cao, Q. Guo, Z.Q. Tan, G.L. Fan, Z.Q. Li, and D. Zhang, *ACS Nano* 9, 6934 (2015).
14. W.J. Kim, T.J. Lee, and S.H. Han, *Carbon* 69, 55 (2014).
15. S.E. Shin, H.J. Choi, J.H. Shin, and D.H. Bae, *Carbon* 82, 143 (2015).
16. X. Du, W.B. Du, Z.H. Wang, K. Liu, and S.B. Li, *Mater. Sci. Eng. A* 711, 633 (2018).
17. S.L. Xiang, X.J. Wang, M. Gupta, K. Wu, X.S. Hu, and M.Y. Zheng, *Sci. Rep. UK* 6, 38824 (2016).
18. C.S. Goh, M. Gupta, J. Wei, and L.C. Lee, *J. Compos. Mater.* 41, 2325 (2007).
19. H.F. Wu, J.C. Li, X.X. Zhang, and L. Geng, *Trans. Mater. Heat Treat.* 39, 14 (2018).
20. Y.S. Yi, Y. Meng, D.Q. Li, S. Sugiyama, and J. Yanagimoto, *J. Mater. Sci. Technol.* 34, 1149 (2018).
21. H. Yan, Y.S. Rao, and R. He, *J. Mater. Process. Technol.* 214, 612 (2014).
22. Q. Chen, G. Chen, L.N. Han, N. Hu, F. Han, Z.D. Zhao, X.S. Xia, and Y.Y. Wan, *J. Alloys Compd.* 656, 67 (2016).
23. H. Asgharzadeh and M. Sedigh, *J. Alloys Compd.* 728, 47 (2017).
24. X. Gao, H.Y. Yue, E.J. Guo, S.L. Zhang, B. Wang, E.H. Guan, S.S. Song, and H.J. Zhang, *Mater. Des.* 94, 54 (2016).
25. H.Y. Xu, Z.S. Ji, M.L. Hu, and Z.Y. Wang, *Trans. Nonferrous Met. Soc.* 22, 2906 (2012).
26. M.H. Nai, J. Wei, and M. Gupta, *Mater. Des.* 60, 490 (2014).
27. K.P. So, I.H. Lee, D.L. Duong, T.H. Kim, S.C. Lim, K.H. An, and H.L. Young, *Acta Mater.* 59, 3313 (2011).
28. L. Zhang, Q.D. Wang, W.J. Liao, W. Guo, W.Z. Li, H.Y. Jiang, and W.J. Ding, *Mater. Sci. Eng. A* 689, 427 (2017).
29. Z.R. Zeng, Y.M. Zhu, R.L. Liu, S.W. Xu, C.H.J. Davies, J.F. Nie, and N. Birbilis, *Acta Mater.* 160, 97 (2018).
30. W.B. Hutchinson and M.R. Barnett, *Scr. Mater.* 63, 737 (2010).
31. S.R. Agnew, D.W. Brown, and C.N. Tome, *Acta Mater.* 54, 4841 (2006).
32. O. Muransky, D.G. Carr, M.R. Barnett, E.C. Oliver, and P. Sittner, *Mater. Sci. Eng. A* 496, 14 (2008).
33. M.R. Barnett, Z. Keshavarz, and X. Ma, *Metall. Mater. Trans.* 37, 2283 (2006).
34. J.W. Luste, M. Thumann, and R. Baumann, *Metal. Sci. J.* 9, 853 (1993).
35. W.S. Miller and F.J. Humphreys, *Scr. Metall. Mater.* 25, 33 (1991).
36. P.B. Li and T.J. Chen, *Powder Metall.* 59, 288 (2016).

Publisher's Note Springer Nature remains neutral with regard to jurisdictional claims in published maps and institutional affiliations.